DOI: 10.1002/adma.200601162

Nanowire Piezoelectric Nanogenerators on Plastic Substrates as Flexible Power Sources for Nanodevices**

By *Pu Xian Gao*, *Jinhui Song*, *Jin Liu*, and *Zhong Lin Wang**

Research applications in biomedical science and technology usually require various portable, wearable, easy-to-use, and/or implantable devices that can interface with biological systems.[1,2] Organic or hybrid organic–inorganic microelectronics and nanoelectronics have long been a possibility.[3–7] However, these devices require a power source, such as electrochemical cells[8] or piezoelectric,[9] thermoelectric,[10] and pyroelectric transducers,[11] to generate or store the electrical energy created through chemical, mechanical, or thermal processes. Finding a suitable power source has remained a major challenge for many devices in bioengineering and medical fields.

ZnO is a typical piezoelectric and pyroelectric inorganic semiconducting material used for electromechanical and thermoelectrical energy conversion. Nanostructures of ZnO,[12] such as nanowires (NWs),[13,14] nanobelts (NBs),[15] nanotubes,[16–18] nanorings,[19] nanosprings,[20,21] and nanohelices,[22] have attracted extensive research interest because of their potential applications as nanoscale sensors and actuators. While most of the current applications focus on its semiconducting properties, only a few efforts have utilized the nanometer-scale piezoelectric properties of ZnO. Using ZnO NW arrays grown on a single-crystal sapphire substrate, we have successfully converted mechanical energy into electrical energy at the nanoscale.[23] A conductive atomic force microscopy (AFM) tip was used in contact mode to deflect the aligned NWs. The coupling of piezoelectric and semiconducting properties in ZnO creates a strain field and charge separation across the NWs as a result of their bending. The rectifying characteristic of the Schottky barrier formed between the metal tip and the NW leads to electrical current generation. This is the principle behind piezoelectric nanogenerators.

The ceramic and semiconducting substrates used for growing ZnO NWs are hard and brittle and cannot be used in applications that require a foldable or flexible power source, such as implantable biosensors. In this Communication, by using ZnO NW arrays grown on a flexible plastic substrate, we demonstrate the first successful flexible power source built on conducting-polymer films. This approach has two specific advantages: it uses a cost-effective, large-scale, wet-chemistry strategy to grow ZnO NW arrays at temperatures lower than 80 °C, and the growth of aligned ZnO NW arrays can occur on a large assortment of flexible plastic substrates. The latter advantage could play an important role in the flexible and portable electronics industry. Various dimensions, shapes, and orientations of ZnO NWs and microwires on flexible plastic substrates have been shown to be capable of producing piezoelectric voltage output, giving a real advantage for energy harvesting using large-scale ZnO NW arrays. The voltage generated from a single NW can be as high as 50 mV, which is large enough to power many nanoscale devices.

The ZnO NWs were grown in solution using a synthetic chemistry approach. Figure 1 shows a series of scanning electron microscopy (SEM) and transmission electron microscopy (TEM) images of typical ZnO NW arrays grown on a conductive plastic substrate. Figure 1a shows a low-resolution, top-down view of the densely aligned NW arrays. The aligned NWs have a uniform diameter of 200–300 nm and a hexago-

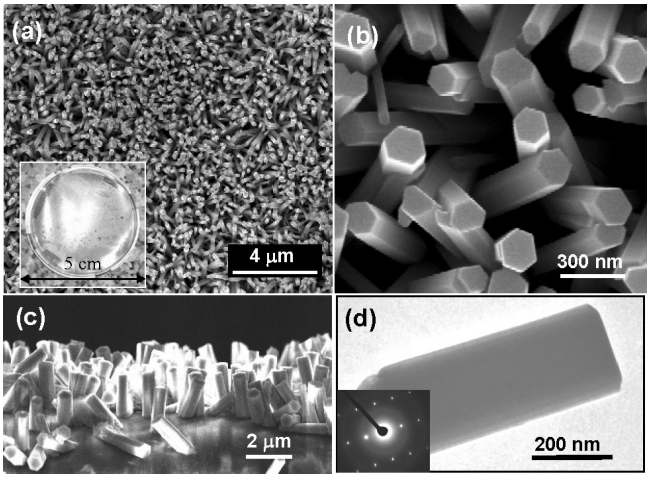

Figure 1. A series of SEM and TEM images of typical ZnO NW arrays grown on a plastic substrate. a) A low-magnification, top-down view of the densely aligned NW arrays and b) a corresponding higher-resolution SEM image. The inset in (a) is an optical image of a sample of NWs on a polymer surface. c) An SEM image of a side view of the sample displaying ZnO NWs aligned normal to the plastic substrate. d) A typical TEM image of an individual ZnO NW; inset is the corresponding electron diffraction pattern of the selected area.

[*] Prof. Z. L. Wang, Dr. P. X. Gao, J. Song, J. Liu
School of Materials Science and Engineering
Georgia Institute of Technology
Atlanta, GA 30332-0245 (USA)
E-mail: zhong.wang@mse.gatech.edu

[**] We acknowledge support from the National Science Foundation, the National Aeronautical and Space Administration (NASA) Vehicle Systems Program, the Department of Defense Research and Engineering (DDR&E), the Defense Advanced Research Projects Agency (DARPA), and CCNE from the NIH.

ADVANCED MATERIALS

nal cross section, as indicated by the magnified SEM image in Figure 1b. The SEM image in Figure 1c displays ZnO NWs ca. 2 μm long aligned perpendicular to the plastic substrate. Figure 1d is a typical TEM image of a ZnO NW that has a diameter of ca. 300 nm. The corresponding electron diffraction pattern indicates that the NW growth direction is [0001] and its side surfaces are $\{2\bar{1}\bar{1}0\}$.

It is worth noting that by controlling reaction conditions such as temperature, concentration, pH value, reaction time, and plastic-substrate surface quality, NWs of different density distributions, dimensionality, and alignment have been fabricated for electrical measurements. Figure 2a and b shows low-resolution and magnified SEM images, respectively, depicting sparsely grown ZnO NW arrays on a plastic substrate. The NWs have a density of ca. 1 μm^{-2} on a Au-coated plastic substrate. The NWs are typically 100–350 nm wide and ca. 1 μm long. The SEM image shown in the inset of Figure 2b is a side view of the NWs aligned perpendicularly to the plastic substrate.

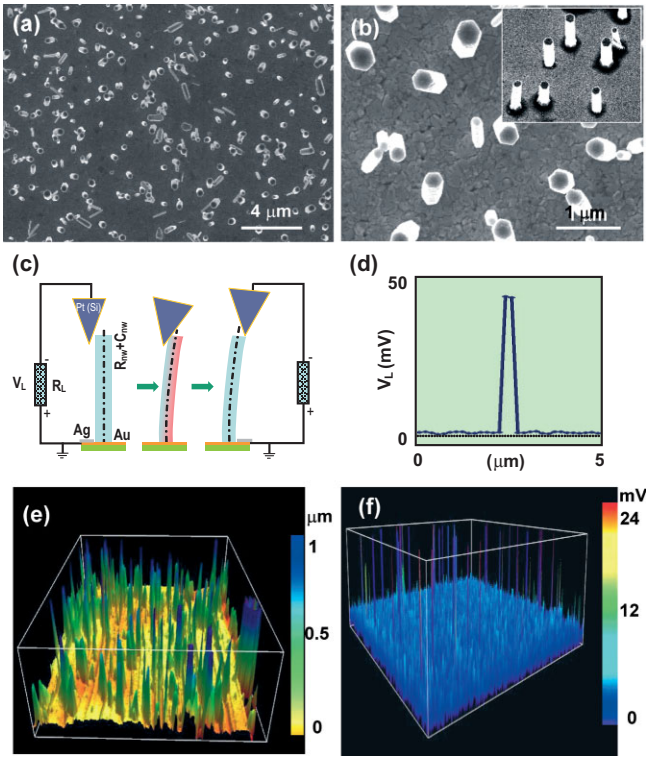

Figure 2. a) A low-magnification and b) a higher-resolution SEM image showing a sparsely grown ZnO NW array on a plastic substrate. c) Schematic illustrating the experimental setup for the conductive AFM measurement of the NW array. Note the polarity of the defined output voltage on the external load. d) A typical voltage output profile for the AFM tip scanning over a single NW on the plastic substrate. e) A 3D plot of the AFM topography image and f) a voltage output profile obtained by scanning the AFM tip over a 40 μm × 40 μm area of aligned ZnO NWs on a plastic substrate.

Figure 2c is a schematic depicting the experimental setup used for measuring the mechanically induced piezoelectric discharge from individual NWs.[23] A conductive Si tip coated with a Pt film with a cone angle of 70° was used for AFM measurements. The rectangular cantilever had a calibrated normal spring constant of 1.857 $N\,m^{-1}$. In the AFM contact mode, a constant normal force of 5 nN was maintained between the tip and sample surface. When the tip was scanned over the top of the ZnO NWs, the tip height was adjusted according to the surface morphology and local contacting force. For the electric contact at the bottom of the NWs, Ag paste was applied to connect the Au film on the plastic substrate surface to the measurement circuit. Connecting Ag and ZnO produces an Ohmic contact.[24] The output voltage across an external load of resistance $R_L = 500$ MΩ was continuously monitored as the tip was scanned over the NWs. In contact mode, as the tip was scanned over the vertically aligned NWs, the NWs were bent consecutively. The tip forced the elastic deflection of the oriented ZnO NWs and produced a charge separation and a voltage drop across the diameter of the NWs, with the stretched and compressed sides having positive and negative piezoelectric potentials, respectively. The center axis of the NW, as indicated by the dotted line, remained neutral.

As the conductive tip was scanned across the neutral axis, a discharge occured when the tip touched the compressed side of the NW. A single NW that has a diameter of 300 nm can produce an output voltage discharge of ca. 45 mV (Fig. 2d), which is the voltage drop across an external resistor converted using the measured electrical current. In fact, the true output voltage should be higher if we consider the inner resistance of the NW. Figure 2d is a typical voltage output for an AFM tip scanning over a single NW. Because of the limited scan speed of the AFM tip in comparison to the discharge time, only two data points were captured around the peak area, which suggests that the true peak could be twice as large as the measured 45 mV shown in this profile.

The scanning speed of the AFM tip was 53.51 $\mu m\,s^{-1}$, and the full width at half maximum (FWHM) of the peak in Figure 2d is 234 nm. Therefore, the lifetime decay constant of the circuit shown in Figure 2c is estimated to be $\tau_c = 4.4$ ms, based on the equation $\tau_c = (R_L + R_{nw})C_{nw}$, where R_L and R_{nw} are the resistances for the external load (500 MΩ) and the ZnO NW, respectively, and C_{nw} is the capacitance of the NW and the measurement system. As previously reported,[23] R_{nw} is negligible in comparison to the external load; thus, the capacitance of the NW can be calculated by $C_{nw} \approx \tau_c / R_L$. The output piezoelectric energy, W_o, for a single pulse is $W_o = 1/2 C_{nw} V_p^2 = \tau_c V_p^2 / 2R_L = 8.9 \times 10^{-15}$ J, where V_p is the peak voltage. Here W_o only represents the harvested electrical energy from the first half cycle of the NW resonance that results from a single touch of the tip to the NW.

Power was calculated based on the average energy generated within the resonance lifetime, and it was assumed that the energy generated for half of the resonance cycles was collected. In this case, the individual NWs are typically 300 nm in diameter, exhibit a hexagonal cross section, and are ca. 1 μm in length. According to mechanical vibration theory,

the first harmonic resonance frequency of the NW can be calculated to be ca. 70 MHz; considering the damping effect in air, the lifetime of a single NW is ca. 50 μs.[25] Therefore, the effective number of cycles required for energy harvesting is about 3500. By considering the decay of the vibration amplitude of a NW for the subsequent resonance, the output power of a single NW is 10–20 pW.

Figure 2e is a 3D plot of a topographic AFM scan of a 40 μm × 40 μm area of the ZnO NW array. The scanning direction is from the front to the back, which can be seen from the raised linear traces on the flexible plastic substrate. Because of the flexibility of the plastic substrate and in spite of the firm adhesion to the Ag paste, the substrate surface profile under tip contact was somewhat wavy. Relative to the plastic substrate, the NW array was revealed to have a height distribution of 0.5–2.0 μm. The corresponding 3D plot of the voltage output image is shown in Figure 2f. There are a number of sharp peaks ranging from 15 to 25 mV that represent voltage outputs. By counting the pulse numbers shown here with respect to the number of NWs in the topography profile in Figure 2e, the ratio of voltage peaks to the number of available NWs is 90:150 or about 60 %, which suggests that the discharge events of the NWs captured by the AFM tip correspond to at least 50 % of the NWs. In fact, because of the limitation in the data-collecting speed of the atomic force microscope, which has a data step size of ca. 156.2 nm in this measurement, the discharge peaks of some NWs were missed, possibly due to poor contact between the tip and the NWs and/or due to multiple contacts with neighboring NWs. It is suggested that both suitable bonding strength between the ZnO NWs and the polymer substrate and a uniform density distribution of NWs in the array might be very important in terms of improving the piezoelectric discharge efficiency. These two issues, together with the power output calculations, will be explored in the following discussions.

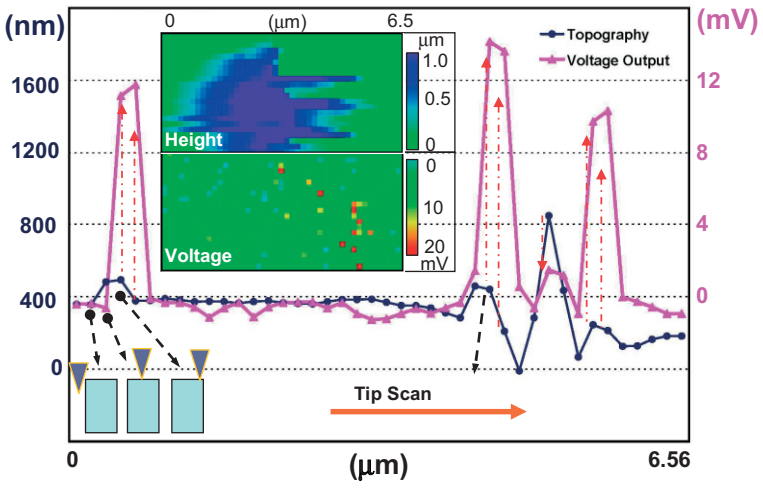

Figure 3. The simultaneously recorded line scanning topography image (blue dotted line) and voltage output profile (pink line) of several aligned ZnO NWs. The inset in the upper part of the figure shows a 2D height profile (top) and a simultaneously recorded voltage output image (bottom) obtained by scanning the tip across an area of 6.5 μm × 3.2 μm. A schematic depicting the tip and NW local contacts is displayed at the bottom left corner for the corresponding locations.

To calculate the total number of NWs that effectively produced electrical energy output, we assumed an average voltage peak height of ca. 20 mV, and the density of ZnO NWs on the plastic substrate was very conservatively estimated to be 1 μm^{-2}. The power density per unit substrate area is ca. 1–2 pW μm^{-2}, that is, 0.1–0.2 mW cm^{-2}, which is large enough to power a variety of devices that operate at lower power consumption, such as microelectromechanical systems (MEMS), nanoelectromechanical systems (NEMS), and other nanoscale devices.

Figure 3 displays simultaneously the recorded scanning height topography (blue line) and voltage-output profile (pink line) for a line scan of the AFM tip across a ZnO NW array. In the scanning range of 6.56 μm, at least four NWs have been contacted based on the topography profile. As registered with the topography profile, the corresponding voltage-output profile also shows four peaks of heights 12, 15, 2, and 10 mV. In each case, the voltage-output peak begins to increase when the AFM tip touches the flat cross section of the NW, and the voltage peak reaches its maximum when the AFM tip reaches the side edge of the top flat cross section of the NW. When the AFM tip starts to cross the central axial line of the NW, the voltage discharge begins, which occurs between two data points corresponding to the center of the discharge peak. When the tip completely releases the NW tip, the discharge is determined by the characteristics of the external circuit. The delay in the voltage peak in reference to the topography profile is entirely consistent with the mechanism presented previously.[23]

The inset in Figure 3 displays the 2D AFM topography image and the corresponding voltage/current output image recorded simultaneously when the AFM tip scans over a 6.5 μm × 3.2 μm area. The height profile in the top image indicates that the local density of the NWs is so large that the AFM tip could not resolve them individually because of the tip size effect; thus, only the surrounding NW edges could be resolved. The corresponding voltage-output profile reveals that the red dots are distributed only at the extreme right-hand side, indicating that the discharge occurs at the end of the tip scan over the NWs. In this case, the high local density of the NW array prevented the deflection event from achieving completion without multiple contacts. Therefore, a reasonable NW density distribution that matches with the tip size and scanning speed would be necessary for improving the voltage-output number.

In our previous report,[23] we studied NWs that were 20–40 nm in diameter and 0.2–0.5 μm in length grown on a sapphire substrate, and we found that a single NW generated ca. 0.5 pW at 10 mV of electrical power using AFM tip deflec-

ADVANCED MATERIALS

tion at a 5 nN contact force. Here, NWs grown on a polymer substrate with diameters of 300 nm and lengths of 1 μm give rise to an output power of ca. 5 pW at 45 mV. This value has improved by an order of magnitude.

To evaluate the power-generating capability of ZnO NW arrays grown on plastic substrates, NW arrays configured differently in terms of dimensions and orientation have been tested to demonstrate the performance of the nanogenerator, and these arrays are shown in Figures 4 and 5. Figure 4a is a top-down view of an as-grown, densely packed, vertically aligned ZnO *microwire* array on a plastic substrate. The microwires are uniform with a width of 1–2 μm and a height of 5–10 μm.

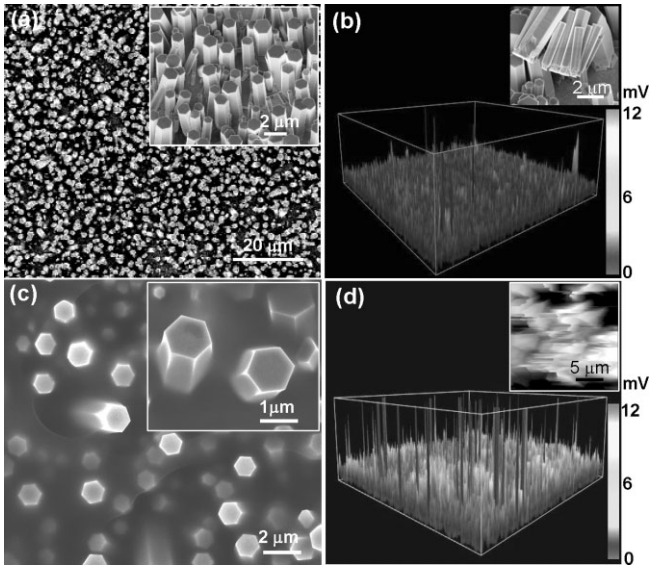

Figure 4. a) An SEM image showing a top-down view of the as-grown, densely packed, vertically aligned ZnO microwire array (inset: a side view showing the alignment of the microwires) on a plastic substrate and b) the corresponding AFM voltage output profile (20 μm × 20 μm). The inset in (b) is an SEM image showing a portion of the microwires pushed down by the AFM tip. c) An SEM image showing a top-down view of ZnO wires immersed in a PMMA coating on a plastic substrate (inset: an enlarged view of the PMMA-encapsulated microwires) and d) the corresponding AFM voltage output profile from AFM measurements (inset: topography image of the 20 μm × 20 μm area).

The SEM image in the inset is a side-on view of the aligned wire array, which reveals a good vertical alignment on the plastic substrate. The microwires are separated by 0.1–1 μm. The substrate surface area covered by the wires is 50–80 % (the surface coverage in the case of Fig. 2 is only ca. 10 %). Under the conductive AFM test, using the same test parameters as those used for the system in Figure 2, we found that the voltage discharge events occurred much less frequently than for the sparsely aligned NWs, simply indicating that a densely packed NW array is not the optimum choice for enhancing the power output of nanogenerators. Figure 4b is the corresponding 3D plot of the voltage image for an area of size 20 μm × 20 μm. We clearly see that only a few (ca. 10) sharp voltage peaks emerge out of the noise level, suggesting that

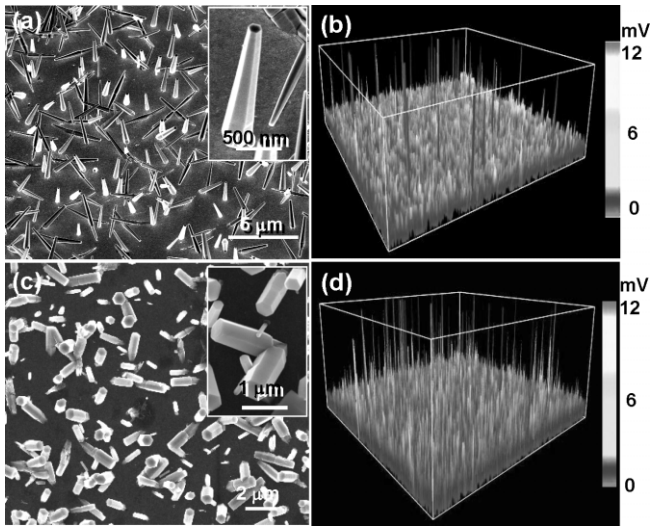

Figure 5. a) A typical SEM image of sparsely grown ZnO nanocones (inset: a magnified view of a single nanocone) and b) the corresponding AFM voltage output profile (20 μm × 20 μm). c) An SEM image of a typical top-down view of a randomly oriented ZnO NW array on a plastic substrate (inset: an enlarged view showing the randomly tilted NWs on a plastic substrate) and d) the corresponding AFM voltage output profile (20 μm × 20 μm).

the small normal tip force (5 nN) may not be sufficiently strong to deflect the ZnO microwires. To find out why only a few peaks were detected in the AFM scan in an area that has at least 50 wires, the tested sample was examined by using SEM. After tip scanning we found that only a few wires were left standing upright on the substrate; most of the wires in the array were pushed down by the AFM tip, as shown in the SEM image in the inset. Several possible reasons may account for this result. First, the adhesion between the Au-coated base and the ZnO microwires could be so weak that it cannot bear the force applied by the AFM tip. The second reason could be that the microwire is too strong to be elastically deformed; once it is pushed by the AFM tip, it tends to be displaced owing to a weak connection to the substrate rather than elastic deformation. Finally, the density of the wires could be so high that there is not much room for the wires to be deflected by the AFM tip without touching neighboring wires; thus, the piezoelectric current, if any, may slowly leak out, resulting in a gradual discharge signal.

To improve the bonding between the wires and the substrate, a poly(methyl methacrylate) (PMMA) coating approximately 200 nm thick was introduced on the substrate after wire growth. Figure 4c shows the ZnO microwire array on a plastic substrate after the PMMA coating. We clearly see that the bottom portion of the wire array has been encapsulated by the PMMA coating (inset). The top portion of the wire array is clean after 10 min of UV irradiation following a spin-coating and soft-baking process. In Figure 4c, the shorter wires have been buried by the PMMA coating, while most of the long microwires are standing on the surface. The result from AFM measurements is shown in Figure 4d. The number

of voltage peaks in an area of 20 μm × 20 μm has increased to ca. 50. The peak voltage output amplitude remains in the range of 6–12 mV. The inset is an AFM topography image of the corresponding microwire array affixed by PMMA. It is clearly seen that the microwires are firmly held onto the plastic substrate during the tip scan, as shown in the topography image, suggesting that by using a reinforcing layer of polymer coating, the NW/substrate connection can be significantly improved.

To determine the effect of NW shape and orientation on power generation, cone-shaped ZnO NWs and randomly oriented ZnO NWs on plastic substrates were grown and used for AFM measurements. Figure 5a shows as-grown, cone-shaped ZnO hexagonal NWs with ca. 50 % vertical alignment on a plastic substrate. The nanocones typically have tip diameters of 100–200 nm, base diameters of 300–500 nm, and lengths of 3–5 μm (inset). Under the conductive tip deflection, only a few voltage output peaks in the range of 6–12 mV are observed (Fig. 5b). Figure 5c is a typical SEM image of the as-grown ZnO NWs oriented randomly on the plastic substrate. The SEM image in the inset reveals the tilted hexagonal NWs rooted at the plastic substrate with dimensions of 200–600 nm in width and 1–2 μm in length. The AFM measurement result is shown in Figure 5d, and it reveals an increased number of voltage output peaks of 6–12 mV, suggesting that as long as there is a way to bend the wires, a voltage/current signal is likely to be generated no matter what kind of orientation the wires adopt with respect to the plastic substrate. This result offers another advantage to energy harvesting utilizing large-scale NW arrays made by using solution-based chemistry.

The lead zirconium titania (PZT) ceramic is the most typical ceramic material for piezoelectric applications, and it has been used for producing output voltage.[26] In comparison to PZT, a NW array grown on a polymer substrate has a number of advantages for generating electricity. First, the NW-based nanogenerators can be subjected to extremely large deformations, both on the NWs and the substrate, indicating that they can be used for flexible electronics as flexible/foldable power sources. Second, the large degree of deformation that the NWs can bear is likely to afford a much larger volume density of power output. Third, in contrast to PZT, ZnO is a biocompatible, "biosafe" material, suggesting that it has a greater potential for use as an implantable power source in the human body. Fourth, the flexibility of the polymer substrate used for growing ZnO NWs makes it feasible to accommodate the flexibility of human muscles so that we can use the mechanical energy (body movement, muscle stretching) in the human body to generate electricity. Finally, ZnO NW nanogenerators can directly produce current because of their enhanced conductivity in the presence of oxygen vacancies.

In conclusion, we have successfully demonstrated that arrays of piezoelectric, semiconducting ZnO NWs grown on flexible plastic substrates can be used to convert mechanical energy into electrical energy using a conductive atomic force microscope. The output discharge voltage from a single ZnO NW can be as large as ca. 45 mV. The estimated piezoelectric-induced electrical power density of the NW array upon deflection of an AFM tip was on the order of milliwatts per centimeter squared, which is large enough to power a variety of MEMS, NEMS, and other nanoscale devices. Various dimensions, shapes, and orientations of ZnO NWs and microwires on flexible plastic substrates have been shown to be capable of producing piezoelectric voltage output, giving a real advantage for energy harvesting using large-scale ZnO NW arrays fabricated by using a wet chemistry approach. The piezoelectric power generators that use ZnO NW arrays on flexible plastic substrates may be able to harvest energy from their environment, such as body movements (e.g., gestures, respiration, or locomotion) and mechanical vibrations, for powering nanodevices and nanosystems. This flexible power source can find potential applications in implantable biosensors and biodetection, wireless self-powered sensors, and self-powering electronic devices.

Experimental

The plastic substrates used were 50 μm thick Kapton polyimide films provided by Dupont. Zinc nitrate hydrate ($Zn(NO_3)_2{\cdot}6\,H_2O$) and hexamethylenetetramine were purchased from Fluka.

Synthesis of Aligned ZnO Nanowires: The aligned ZnO NWs arrays were grown on a plastic film using a solution-based method [27–31]. Serving as one of the electrodes for a later electrical connection and also functioning as uniform nucleation sites for NW growth, a thin, ca. 100 nm, layer of Au was deposited on the plastic substrate by using thermal evaporation at 0.3-0.5 $Å\,s^{-1}$ before the hydrothermal growth of ZnO NW arrays. The growth of ZnO NWs was conducted by suspending the Au-coated plastic substrate in a Pyrex glass bottle filled with an equal molar aqueous solution of $Zn(NO_3)_2{\cdot}6\,H_2O$ (0.01–0.04 M) and hexamethylenetetramine (0.01–0.04 M) at temperatures between 60 and 80 °C. The temperature, solution concentration, reaction time (1–72 h), and substrate surface quality were optimized for growing NW arrays with controlled dimensions and orientation. After reaction, the plastic substrates were removed from the solution, rinsed with deionized water, and dried in air at 60–80 °C overnight.

Morphology and Structure Characterization: The as-grown ZnO NWs were characterized with a scanning electron microscope (LEO 1530 and 1550 FEG at 5 and 10 kV) and a transmission electron microscope (Hitachi HF-2000 at 200 kV).

Electrical Measurement: Electrical measurements on the aligned NW array were conducted using an atomic force microscope (Molecular Force Probe MFP-3 from Asylum Research). The detailed methodology for generating electricity using a conductive AFM tip was reported previously [23].

Nanowire/Plastic Substrate Interconnection Reinforcement: To reinforce the interconnection between the Au-coated plastic substrate and the ZnO microwire array, a matrix of spin-coated PMMA ca. 200 nm thick was used to encapsulate the bottom portion of the NW array. Four percent of 495 PMMA photoresist in anisole was used. The photoresist was spun onto the substrate at a speed of 3000 rpm for 35 s. The substrate was then baked at 120 °C for 1 min to remove the solvent. UV light with a wavelength of 325 nm and an intensity of 3.1 $mW\,cm^{-2}$ was utilized to expose the as-coated sample for 10 min to crosslink the PMMA photoresist and also to expose the microwire tip portions for late circuit connection in the AFM measurement.

Received: May 29, 2006
Revised: August 13, 2006
Published online: December 12, 2006

ADVANCED MATERIALS

[1] M. Billinghurst, T. Starner, *IEEE Computer* **1999**, *32*, 57.
[2] D. De Rossi, A. Della Santa, A. Mazzoldi, *Mater. Sci. Eng. C* **1999**, *7*, 31.
[3] R. F. Service, *Science* **2003**, *301*, 909.
[4] Q. M. Zhang, V. Bharti, X. Zhao, *Science* **1998**, *280*, 2101.
[5] A. J. Heeger, *J. Phys. Chem. B* **2001**, *105*, 8475.
[6] S. Ashley, *Sci. Am.* **2003**, *10*, 52.
[7] Q. M. Zhang, H. Li, M. Poh, F. Xia, Z. Y. Cheng, H. Xu, C. Huang, *Nature* **2002**, *419*, 284.
[8] X. Yu, J. B. Bates, G. E. Jellison, Jr., F. X. Hart, *J. Electrochem. Soc.* **1997**, *144*, 524.
[9] N. S. Shenck, J. A. Paradiso, *IEEE Micro* **2001**, *21*, 30.
[10] R. Venkatasubramanian, E. Siivola, T. Colpitts, B. O'Quinn, *Nature* **2001**, *413*, 597.
[11] D. Setiadi, H. Weller, T. D. Binnie, *Sens. Actuators, A* **1999**, *76*, 145.
[12] Z. L. Wang, X. Y. Kong, Y. Ding, P. X. Gao, W. L. Hughes, R. Yang, Y. Zhang, *Adv. Funct. Mater.* **2004**, *14*, 943.
[13] Y. N. Xia, P. D. Yang, Y. G. Sun, Y. Y. Wu, B. Mayers, B. Gates, Y. D. Yin, F. Kim, Y. Q. Yan, *Adv. Mater.* **2003**, *15*, 353.
[14] M. H. Huang, Y. Y. Wu, H. Feick, N. Tran, E. Weber, P. D. Yang, *Adv. Mater.* **2003**, *13*, 113.
[15] Z. W. Pan, Z. R. Dai, Z. L. Wang, *Science* **2001**, *291*, 1947.
[16] J. J. Wu, S. C. Liu, C. T. Wu, K. H. Chen, L. C. Chen, *Appl. Phys. Lett.* **2002**, *81*, 1312.
[17] Y. J. Xing, Z. H. Xi, Z. Q. Xue, X. D. Zhang, J. H. Song, R. M. Wang, J. Xu, Y. Song, S. L. Zhang, D. P. Yu, *Appl. Phys. Lett.* **2004**, *83*, 1689.
[18] P. X. Gao, C. S. Lao, Y. Ding, Z. L. Wang, *Adv. Funct. Mater.* **2006**, *16*, 53.
[19] X. Y. Kong, Y. Ding, R. S. Yang, Z. L. Wang, *Science* **2004**, *303*, 1348.
[20] X. Y. Kong, Z. L. Wang, *Nano Lett.* **2003**, *3*, 1625.
[21] P. X. Gao, Z. L. Wang, *Small* **2005**, *1*, 945.
[22] P. X. Gao, Y. Ding, W. J. Mai, W. L. Hughes, C. S. Lao, Z. L. Wang, *Science* **2005**, *309*, 1700.
[23] Z. L. Wang, J. H. Song, *Science* **2006**, *312*, 242.
[24] J. H. Song, J. Zhou, Z. L. Wang, *Nano Lett.* **2006**, *6*, 1656.
[25] J. Zhou, C. S. Lao, P. X. Gao, W. J. Mai, Z. L. Wang, N. S. Xu, *Solid State Commun.* **2006**, *139*, 222.
[26] S. R. Platt, S. Farritor, H. Haider, *IEEE/ASME Trans. Mechatronics* **2005**, *10*, 240.
[27] L. Vayssieres, *Adv. Mater.* **2003**, *15*, 464.
[28] S.-Y. Chen, C.-C. Lin, S.-Y. Cheng, *J. Cryst. Growth* **2005**, *283*, 141.
[29] C. Y. Lee, S. Y. Li, P. Lin, T. Y. Tseng, *J. Nanosci. Nanotech.* **2005**, *5*, 1088.
[30] J. B. Cui, C. P. Daghlian, U. J. Gibson, R. Pusche, P. Geithner, L. Ley, *J. Appl. Phys.* **2005**, *97*, 44 315.
[31] T. L. Sounart, J. Liu, J. A. Voigt, J. W. P. Hsu, E. D. Spoerke, Z. Tian, Y. B. Jiang, *Adv. Funct. Mater.* **2006**, *16*, 335.